Journal of Computational Science &Engineering 52 (2021) 1200-1206

Available at http://www.asocse.org ISSN 1710-4068

Research on Thermodynamic Characteristics of Tube Weld in Hydraulic Cylinder based on ABAQUS

Jitao Chen, Haiyan Song, Jixin Liu, Weiwei Ge

Qingdao Huanghai University, China

Abstract: **Welding is one of the most important processes for processing and repairing of hydraulic cylinders. The thermodynamic properties of welded joints have important influence on cylinder dimension stability, residual stress and strength. The thermodynamic characteristics of the weld are studied by means of theoretical analysis, finite element numerical simulation and metallographic analysis. According to the theory of welding thermodynamics, the heat conduction equation of one dimension and multidimensional is analyzed, the boundary condition is established, and the heat transfer equation to be solved is expressed. Based on the analysis of the temperature field under the instantaneous fixed heat source, the method of solving the differential equation of heat conduction is obtained. According to the different effects of the welding heat source, the welding thermal cycling phenomenon at different positions of the weld is analyzed. Based on PRO/E, a cylinder connection assembly drawing is established. The coupled model of temperature and displacement is established by ABAQUS. The transient field variable characteristics and output characteristics of the welded joint of cylinder are obtained. In order to obtain the thermal effect of the weld, the metallographic structure and metallographic analysis and research of weld area are also carried out. It shows that the mechanical property that inferred by metallographic analysis is in accordance with simulation research.**

Keywords: Welding; Thermodynamics; Finite element; Boundary conditions

Received 26 October 2020, Revised 22 November 2020, Accepted 28 December 2020

1.Introduction

The processing technology of hydraulic cylinder mainly consists of welding and machining. Among them, welding method is widely used because of its simple construction, good versatility, high processing efficiency and high strength after welding. In the welding process, the performance of the weld directly determines the mechanical properties of the cylinder, and the characteristics of the temperature field and stress field of the weld have a key impact on the welding effect [1]. Because the cylinder is a precise matching element, the requirement for welding quality is high. Therefore, tungsten argon arc welding is applied mostly. After welding, the quality is high and the oxidation degree is small [2]. However, due to the influence of high temperature during welding, the size of the cylinder is unstable, and the residual thermal stress has a key impact on the strength, life and reliability of cylinder parts. The control method of the deformation and residual thermal stress after welding process optimization to become the key point of the cylinder quality problem. It has great significance to improve the cylinder tube quality and reduce the failure rate to improve the economic efficiency through the study of the cylinder tube weld.

Numerical simulation is a very effective method for the study of welding phenomena and nature, which is based on the establishment of a consistent model and boundary conditions, to solve and analyze the welding process and rules. It can achieve the prediction of welding deformation and have great significance for the optimization of welding process. Image microanalysis is one of the most important means of welding analysis, which is mainly used to analyze the structure of the material by micro technology. The instruments used for image analysis of materials microstructure include metallographic microscope, image analyzer, micro hardness tester, super deep field 3D high speed microscope system, scanning electron microscope and so on.

2.Control equation and boundary of heat transfer in welding

2.1 Heat generation condition and heat transfer equation

In the thermodynamic study of welding joint, the control equation of analytical method [3] consists of four parts: unsteady state term, convection term, diffusion term, source term. When studying the establishment of discrete equations and methods, in order to avoid complicating, it is not necessary to focus on complete equations, on the other hand, extract one item from the same type as a representative to analyze the unsteady convection diffusion equation. In the numerical computation research of convection heat transfer [4], the one-dimensional control equation of x direction is widely used. It includes two kinds with non-conserved and conserved ones as shown in Eq.1 and Eq.2.

$$\rho\frac{\partial\phi}{\partial\tau}+\rho u\frac{\partial\phi}{\partial x}=\frac{\partial}{\partial x}(\Gamma\frac{\partial\phi}{\partial x})+S \qquad (1)$$

$$\frac{\partial(\rho\phi)}{\partial\tau}+\frac{\partial(\rho u\phi)}{\partial x}=\frac{\partial}{\partial x}(\Gamma\frac{\partial\phi}{\partial x})+S \qquad (2)$$

2021@ The American Computational Science Society. All rights reserved.

Available at http://www.asocse.org ISSN 1710-4068

Where φ is generalized variables, ρ is the density of the material, τ is the time, u is air flow rate, c is the specific heat of welding, S welding heat source for heat flux, Γ is generalized heat transfer coefficient, $\Gamma = \lambda / c$. where λ is the coefficient of heat conduction.

Since S is a generalized source term, it is not necessarily the real source of physics that the amount of everything that cannot be attributed to the non-stable, convection and diffusion terms. Set h as a convective heat transfer coefficient for heat conduction problems as follows.

$$\frac{\partial(\rho h)}{\partial \tau} = \frac{\partial}{\partial x}(\frac{\lambda}{c}\frac{\partial h}{\partial x}) + S \qquad (3)$$

Satisfied in one dimensional continuous body as follows.

$$\rho c\frac{\partial t}{\partial \tau} = \frac{\partial}{\partial x}(\lambda\frac{\partial t}{\partial x}) + S \qquad (4)$$

Convection heat transfer equation can be expressed as follows.

$$\frac{\partial(\rho h)}{\partial t} + \frac{\partial(\rho h\ )}{\partial x} = \frac{\partial}{\partial x}(\frac{\lambda}{c}\frac{\partial h}{\partial x}) + S \qquad (5)$$

In order to accurately analyze the model, the control equation [5] can be deduced in the multidimensional space of xyz according to the one-dimensional control equation. The governing differential equation can be expressed as conservation principle.

$$\frac{\partial T}{\partial t} = \frac{\lambda}{c\rho}(\frac{\partial^2 T}{\partial x^2} + \frac{\partial^2 T}{\partial y^2} + \frac{\partial^2 T}{\partial z^2}) + \frac{1}{c\rho}\frac{\partial Q_v}{\partial t} \qquad (6)$$

Where T is temperature dependent on time, and Q_v is the energy dissipation value per unit volume.

1.2 Boundary condition

When z=0 (arc covered area), the heat flow q(r) is welded to the work piece for heat welding as follows.

$$q(r) = \frac{\eta_h IU}{2\pi\sigma_q^2}\exp(-\frac{r^2}{2\sigma_q^2}) \qquad (7)$$

Where I is the input current in the welding process, U is the input voltage, and r is the heat influence radius, η_h is the heat output efficiency of the welding.

In the welding process, when the weld is dissipated by convection heat transfer and heat radiation, the weld on the interface of solid and solid phase is satisfied when it is dissipated through the convection heat transfer and heat radiation [6].

$$u = -u_0, v = 0, w = 0 \qquad (8)$$

$$\mu\frac{\partial v}{\partial z} = -\frac{\partial \sigma}{\partial T}\frac{\partial T}{\partial y}$$
$$\mu\frac{\partial u}{\partial z} = -\frac{\partial \sigma}{\partial T}\frac{\partial T}{\partial x} \qquad (9)$$

In the process of boundary condition treatment, it is reasonable in many cases to replace the finite size with a simplified infinite extension body. Especially, the larger size of the member in the corresponding direction, the shorter heat transmission cycle (heating and cooling) and the lower the thermal diffusivity are appeared. However, when there is a large deviation between the geometric size of the component and the infinite expansion body, there will be a great deviation and even an insoluble contradiction.

In the welding process of the cylinder, the wall temperature changes with the movement of the welding heat source. With the conduct of heat conduction and heat transfer, the temperature of the cylinder first increases and then decreases. With the processing of the next welding path, the temperature changes around the beginning.

3.Thermodynamic properties research of numerical simulation

3.1 The establishment of a finite element model

The welding technology of outer cylinder is very representative, no matter from material, heat treatment or weld quality and strength. Therefore, the paper studies the girth welding technology of outer cylinder. This paper analyzes the connection structure of the outer cylinder of the schematic as shown in Fig.1, and the analysis model is established based on Pro/E.

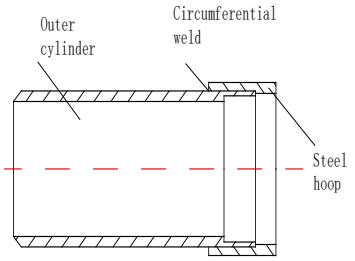

Fig.1 Diagram of outer cylinder connection

The weld of the cylinder is a circumferential weld, and its boundary constraints are more complex than that of the ordinary welds. As the weld is multi welded, each welding will preheat the parent material, and each preheating will result in a certain residual stress. The finite element numerical simulation can calculate the characteristics of the residual stress changing with time, providing a favorable technical support and basis for the

2021@ The American Computational Science Society. All rights reserved.

Available at http://www.asocse.org ISSN 1710-4068

post weld stress relief and welding process optimization [7]. ABAQUS is one of the finite element analysis software with many engineering applications. It can deal with engineering problems in different industries and fields. It not only achieves simple linear analysis, but also realizes complex nonlinear system analysis.

Tab.1 Material properties

Temperature / ℃	20	500	1000	1500	2000
Modulus of elasticity / Pa	2.11e11	1.8e11	0.9e11	0.4e11	0.39e11
Poisson ratio	0.28	0.28	0.28	0.28	0.28
Density / kg/ m^3	7800	7800	7800	7800	7800
Coefficient of linear expansion / 1/℃	1.54e-5	1.95e-5	1.88e-5	1.86e-5	1.84e-5
Specific heat capacity / J/ (kg·℃)	460	530	670	660	800
Heat conduction coefficient / W/ (m·℃)	1.67e-5	1.33e-5	1e-5	1.17e-5	4.7e-5
Yield strength / Pa	1.2e9	0.93e9	0.44e9	0.07e9	0.007e9
Shear modulus / Pa	1.5e10	1.1e10	0.6e10	0.2e10	0.4e10

In ABAQUS, the first analysis step is setting the material properties, which is choosing Q345. In order to get more accurate calculation values and fully consider the relationship between material parameters and temperature as shown in Tab.1. In terms of mesh generation, unit type selects C3D8T unit with temperature and displacement coupling characteristics, which is a hexahedron element with eight nodes. It can achieve three direction linear displacement and temperature solution. In order to divide the mesh with higher quality and improve the operation accuracy, the elements are partitioned on the shoulder position, and the hexahedron swept form is used to complete the mesh generation. Finally, the meshing map is obtained, as shown in Fig. 2.

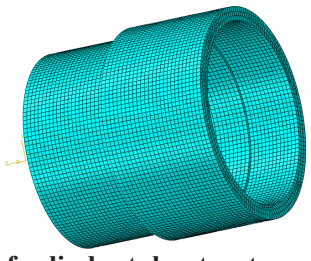

Fig.2 Mesh of cylinder tube structure

3.2 Boundary setting

During the analysis of step setting, the implicit algorithm is adopted, and the transient temperature displacement coupling calculation method is selected with total time of 180s. The incremental step is automatically incremented, considering the characteristics of nonlinearity, the expansion and creep factors are added. In the contact property, mainly two parts contact are set up, including outer tube outer surface and inner steel cylindrical end surface,

2021@ The American Computational Science Society. All rights reserved.

Available at http://www.asocse.org ISSN 1710-4068

with contact types of hard contact. Between the outer cylinder and the steel hoop, the effects of thermal radiation are considered as heat transfer coefficient of 5% in welding process [8~10]. The thermal expansion will be calculated with the coupling method of temperature-displacement step. In the convective heat transfer setting, the heat transfer coefficient of the film is set to 50 and the reference temperature is 20 C according to the natural convection.

3.3 Analysis of field variable results

Through the continuous iteration of 103 incremental steps, the results of the numerical simulation are shown in Fig.3~Fig.9 respectively. In order to facilitate internal analysis, the model is set half-cut, in which Fig.3~Fig.6, and Fig.7~Fig.9 is the analysis of the cloud images at the final 180s moment.

Fig.3 is the transient temperature field at 104th second, it can be seen in the figure that the highest temperature of the time is still in the distance near the weld position. This is because the heat source has just stopped in the heat input [11~13], at this time, the minimum temperature is 320℃.

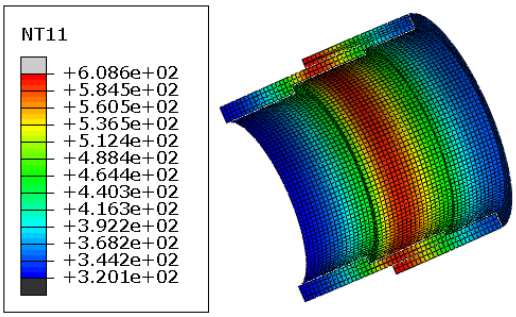

Fig.3 Transient temperature field (104s time)

Fig.4 is the transient stress field at the 104th second, it can be seen from the figure that the maximum stress is located at the contact position for outer surface and the inner steel shaft shoulder. Due to the influence of the temperature field, the thermal expansion occurred. The outer end surface of the cylinder by the positioning effect of steel in the shoulder, hinder the free deformation, resulting in stress concentration.

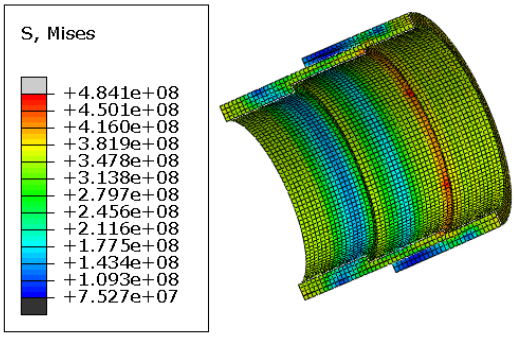

Fig.4 Transient stress field (104s time)

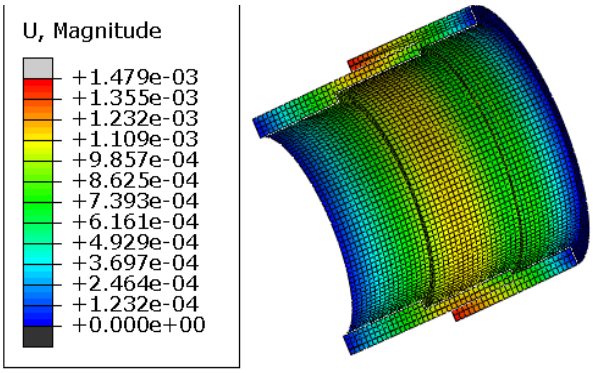

Fig.5 Transient displacement field (104s time)

Fig.5 shows the transient displacement field at the moment of 104th second. It can be seen from the figure that the largest distribution location is adjacent to the weld location. The thermal expansion is the strongest because of the longest continuous high temperature time and no coercive displacement constraints. In the actual production, the method of increasing the tighten rigidity can be achieved in this position to reduce the deformation amount.

Fig.6 is the distribution cloud map of the heat flux vector at the time of 104th second. From the chart, it can be seen that when the heat input stops, the heat flux mainly propagates in the form of heat conduction. The heat flux of the weld zone is greatly reduced, and the heat is mainly convection heat transfer and heat conduction.

Fig.7 is the transient temperature field at 180th second, it can be seen in the figure that the temperature field tends to be balanced after heat conduction and convection heat transfer. The highest temperature is 346 ℃, and the lowest temperature is 336 ℃. The temperature at the thick wall is slightly higher than that at the thin wall.

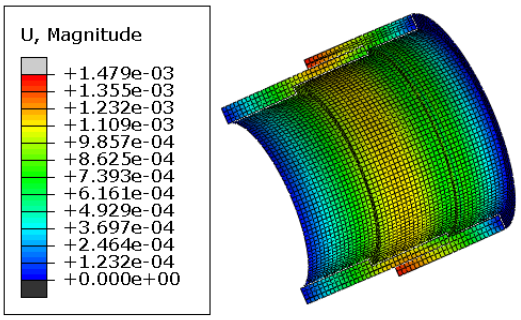

Fig.6 Transient heat flux field (104s time)

2021@ The American Computational Science Society. All rights reserved.

Available at http://www.asocse.org ISSN 1710-4068

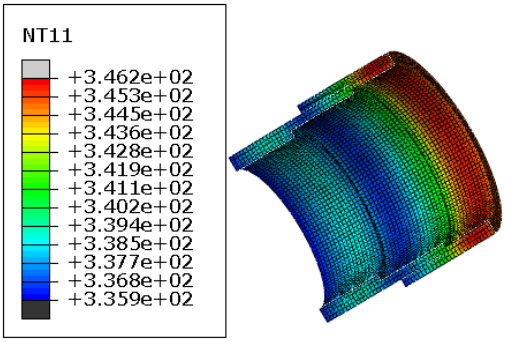

Fig.7 Transient temperature field (180s time)

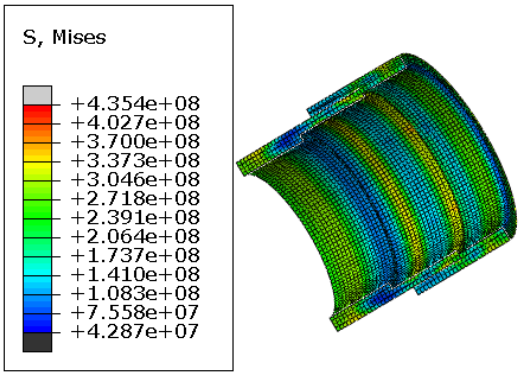

Fig.8 Transient stress field (180s time)

Fig.8 is the transient stress field at the 180th second, it can be seen from the figure that the maximum and minimum value is still a difference of ten times the magnitude of the thermal stress at the end analysis moment. Due to thermal expansion resulting in a large number of residual stress, the maximum stress position is still in the contact position of end face and the outer cylinder hoop in the shoulder, but the phenomenon of stress concentration was significantly improved.

Fig.9 shows the transient displacement field at the moment of 180th second. It can be seen from the figure that the maximum deformation decreases compared with the 104s time. Due to the elastic deformation of the material affected by the temperature, there is a certain rebound effect after the temperature is reduced.

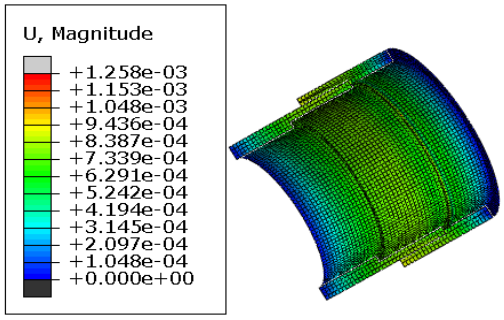

Fig.9 Transient displacement field (180s time)

4. Metallographic characteristics analysis in weld zone

During the vicinity of the fusion zone, the temperature is high and the cooling rate is fast, and a large number of Soxhlet, bainite and ferrite are generated. The welding area is in an overheated state. The temperature in the area is relatively high, and the residence time is relatively long under high temperature. The superheated structure formed after cooling is relatively large, as shown in Fig. 10. Because of the problem of segregation, inclusion of cementite and pearlite of Widmanstatten structure in the overheated zone.

Fig.11 is a metallographic map of the fusion zone. The right side is the weld area, and the nearest one is the semi melting zone near the fusion line. As a hot spot, the heating temperature in the area is close to the melting point of the material. Due to the relatively long residence time at high temperature, the superheated structure formed by cooling has larger grains.

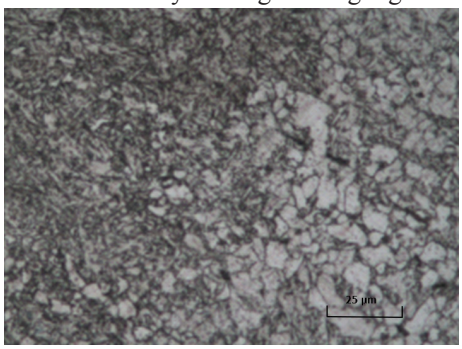

Fig.10 Superheated zone segregation (400×)

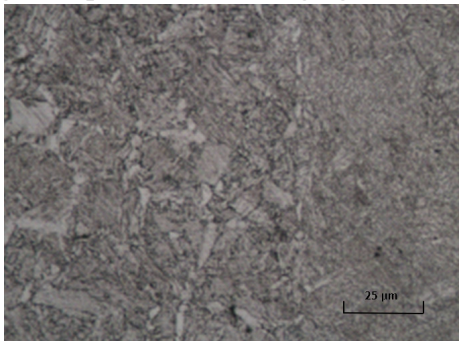

Fig.11 Weld fusion zone organization (400×)

The sampling microstructures in all weld areas are located in the center line of the weld. There is an obvious symmetry distribution in the microstructure of the weld zone, and the surface of the weld is almost superheated, as shown in Fig. 10. According to the grain refinement of the weld surface at a certain distance, it is gradually transferred to a part of the normalizing structure and phase transition, as shown in Fig.11. Due to the rapid cooling rate of the liquid metal in the welding process, the coarser grain appeared in the recrystallization.

2021@ The American Computational Science Society. All rights reserved.

Available at http://www.asocse.org ISSN 1710-4068

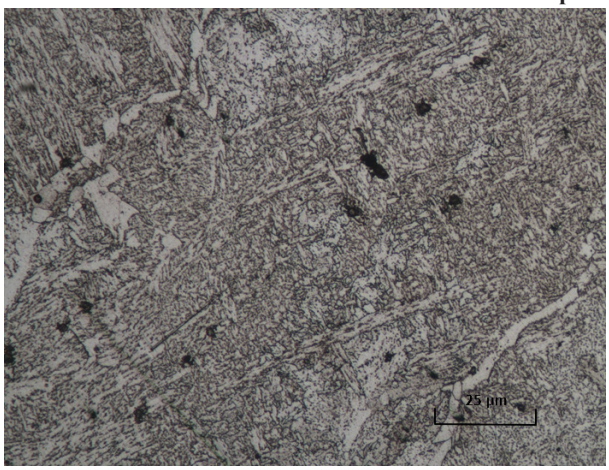

Fig.12 Weld superheated zone (400×)

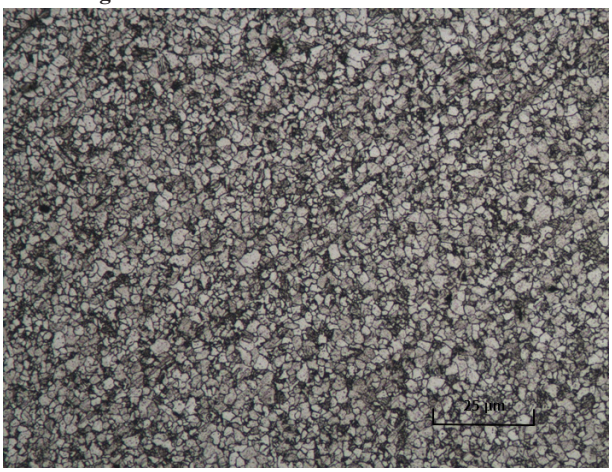

Fig.13 Weld seam normalizing zone (400×)

The proportion of main alloying elements is shown in Tab.2. The main factor affecting the weldability is chemical composition. Among all kinds of elements, carbon has the most obvious influence. Most of the other alloy elements are not conducive to welding, but their influence is generally much smaller than that of carbon. The carbon content in steel increases, the hardening tendency increases, and the plasticity decreases, and welding cracks are easily produced. Therefore, the carbon equivalent method can be used to estimate the weldability of the weldable steel. Sulfur and phosphorus have a great influence on the welding performance of steel, and they are strictly limited.

Tab.2 Proportion of main alloying elements

Alloying element	C	Si	Mn	P	S
Content/ %	≤0.2	≤0.55	1~1.6	≤0.045	≤0.045

5.Conclusions

In this paper, the heat conduction and convection heat transfer in the welding process are analyzed theoretically. In the process of dealing with the boundary conditions, the simplified infinite expansion body is used to replace the finite size, and the heat transfer control equation and boundary condition of the weld are expressed in the form of heat conduction differential equation. Based on the finite element method, the temperature field and stress field of the weld are analyzed, and the characteristics of field variables and the output characteristics of the process are obtained.

Reference

[1] Lu F, Yao S, Lou S, et al. Modeling and finite element analysis on GTAW arc and weld pool[J]. Computational Materials Science, 2004, 29(3):371-378.

[2] Mochizuki M. Numerical analysis of welding residual stress and its verification using neutron diffraction measurement[J]. Journal of Engineering Materials & Technology, 2000, 122(1):98-103.

[3] D. Rudland, Y. Wang,W. Norris. Development of circumferential through-wall crack K-solutions for control rod drive mechanism nozzles[J].International Journal of Pressure Vessels Piping, 2004,81:961–971.

[4] Teng T L, Lin C C. Effect of welding conditions on residual stresses due to butt welds[J]. International Journal of Pressure Vessels & Piping, 1998, 75(12):857-864.

[5] Bachorski, Dean Deng, Shoichi Kiyoshima. Investigations on welding residual stresses in penetration nozzles by means of 3D thermal elastic plastic FEM and experiment. Computational Materials Science, 2009, 45:1031-1042.

[6] Deng D, Murakawa H. Numerical simulation of temperature field and residual stress in multi-pass welds in stainless steel pipe and comparison with experimental measurements[J]. Computational Materials Science, 2006, 37(3):269-277.

[7] Lindgren L, Karlsson L. Deformations and stresses in welding of shell structures[J]. International Journal for Numerical Methods in Engineering, 1988, 25(2):635-655.

[8] Tsai K V, Maksimkin O P, Turubarova L G.

2021@ The American Computational Science Society. All rights reserved.

Available at http://www.asocse.org ISSN 1710-4068

Validated residual stress profiles for fracture assessments of stainless steel pipe girth welds[J]. International Journal of Pressure Vessels & Piping, 2007, 84(4):195-222.

[9] Inoue T. Metallo-Thermo-Mechanics : Application to Phase Transformation incorporated Processes[J]. Transactions of Jwri, 1996, 25(2):69-87.

[10] Gery D, Long H, Maropoulos P. Effects of welding speed, energy input and heat source distribution on temperature variations in butt joint welding[J]. Journal of Materials Processing Tech, 2005, 167(2):393-401.

[11] Goldak J, Chakravarti A, Bibby M. A new finite element model for welding heat sources[J]. Metallurgical Transactions B, 1984, 15(2):299-305.

[12] Chang W S, Na S J. A study on the prediction of the laser weld shape with varying heat source equations and the thermal distortion of a small structure in micro-joining[J]. Journal of Materials Processing Technology, 2002, 120(1–3):208-214.

[13] Ronda J, Oliver G J. Consistent thermo-mechano-metallurgical model of welded steel with unified approach to derivation of phase evolution laws and transformation-induced plasticity[J]. Computer Methods in Applied Mechanics & Engineering, 2000, 189(2):361-418.

2021@ The American Computational Science Society. All rights reserved.